ACS Photonics

Letter

Cite This: ACS Photonics 2019, 6, 59−65

pubs.acs.org/journal/apchd5

Power- and Spectral-Dependent Photon-Recycling Effects in a Double-Junction Gallium Arsenide Photodiode

He Ding,[†] Hao Hong,[‡] Dali Cheng,[§] Zhao Shi,[§] Kaihui Liu,[‡] and Xing Sheng*,[§]

[†]School of Optics and Photonics, Beijing Institute of Technology, Beijing 100081, China

[‡]State Key Laboratory for Mesoscopic Physics, Collaborative Innovation Center of Quantum Matter, and School of Physics, Peking University, Beijing 100871, China

[§]Department of Electronic Engineering and Beijing National Research Center for Information Science and Technology, Tsinghua University, Beijing 100084, China

Supporting Information

ABSTRACT: Photon-recycling effects improve radiative efficiencies of semiconductor materials and play important roles in the design of high-performance optoelectronic devices. Conventional research mostly studies the impact of photon-recycling on the voltage of photodiodes. Here we systematically analyze the photon response of a microscale gallium-arsenide (GaAs)-based double-junction photodiode. In such a device, the current-matching condition between two subcells is determined by their photon coupling. Photodynamics in the device is examined and reveals the material's internal quantum efficiencies. By leveraging photon distributions inside the device, we discover that its photocurrent and spectral responses are highly dependent on the illumination intensity. Consistent with theoretical analyses, the device's photocurrents exhibit linear and superlinear power-dependent characteristics under near-infrared and violet-blue illuminations, respectively. Because of the strongly enhanced photon-recycling effects under strong illumination, broadband photon responses (external quantum efficiency close to 50% from 400 to 800 nm) could be achieved in such a strongly current mismatched GaAs dual-junction device. The understanding of photon processes in such devices would offer routes to the design of high-performance photodetectors and solar cells.

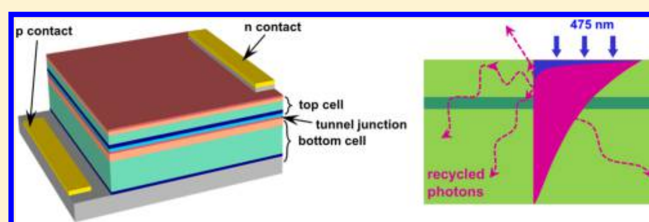

KEYWORDS: *photon recycling, gallium arsenide, photovoltaics, photodetectors, multijunction*

Understanding and engineering optical processes in semiconductor materials are critically important to realize high-performance optoelectronic devices such as photovoltaic (PV) cells, photodetectors, light-emitting diodes (LEDs), and lasers.[1,2] In luminescent semiconductors, photon absorption, re-emission, and self-absorption processes, which are also known as the photon-recycling effects, are of tremendous interest in the study of photon receivers. In particular, remarkable results have been recently demonstrated on III−V and halide-perovskite-based semiconductors, in which improved photon-recycling effects lead to a single-junction or multijunction PV cells with ultrahigh power-conversion efficiencies.[3−7] In these PV cells, enhanced photon-recycling effects increase the open-circuit voltages (V_{oc}), making cell operation approach the detailed balance limit.[8−11] In general, photon-recycling effects are mostly explored under standard one-sun illumination in PV cells, where various strategies like reflector optimization and light-trapping design have been implemented to manipulate the internally radiated photons.[12−14] Meanwhile, optoelectronic properties (quantum efficiencies, carrier lifetimes, etc.) of semiconductor materials and devices are dependent on the wavelength and the power of the incident light,[15,16] of which the influences on photon-recycling are, however, less investigated. In particular, in multijunction devices, the photon processes vary under different current-matching conditions.[7,17] In this Letter, we examine the photon-recycling process in a thin-film microscale gallium-arsenide (GaAs)-based double-junction photodiode. Photon and carrier-transport behaviors under irradiation at various wavelengths and intensities are experimentally and analytically studied. In such a device, we discover that incident wavelengths affect the current-matching conditions, which lead to varied photon-recycling effects. Under violet-blue (400−480 nm) and near-infrared (near-IR) (∼800 nm) illuminations, the output currents exhibit remarkably different dependences on incident powers. These results suggest that photon-recycling effects play a vital role in the optoelectronic device design.

RESULTS AND DISCUSSION

Figure 1a schematically illustrates the device layout of a fabricated thin-film GaAs double-junction photodiode used in this study. The epitaxial device structure contains two GaAs-based pn diodes connected with an ultrathin (∼22 nm) GaAs-

Received: October 9, 2018
Published: January 2, 2019

Downloaded via TSINGHUA UNIV on January 16, 2019 at 08:26:04 (UTC).
See https://pubs.acs.org/sharingguidelines for options on how to legitimately share published articles.

© 2019 American Chemical Society

DOI: 10.1021/acsphotonics.8b01404
ACS Photonics 2019, 6, 59−65

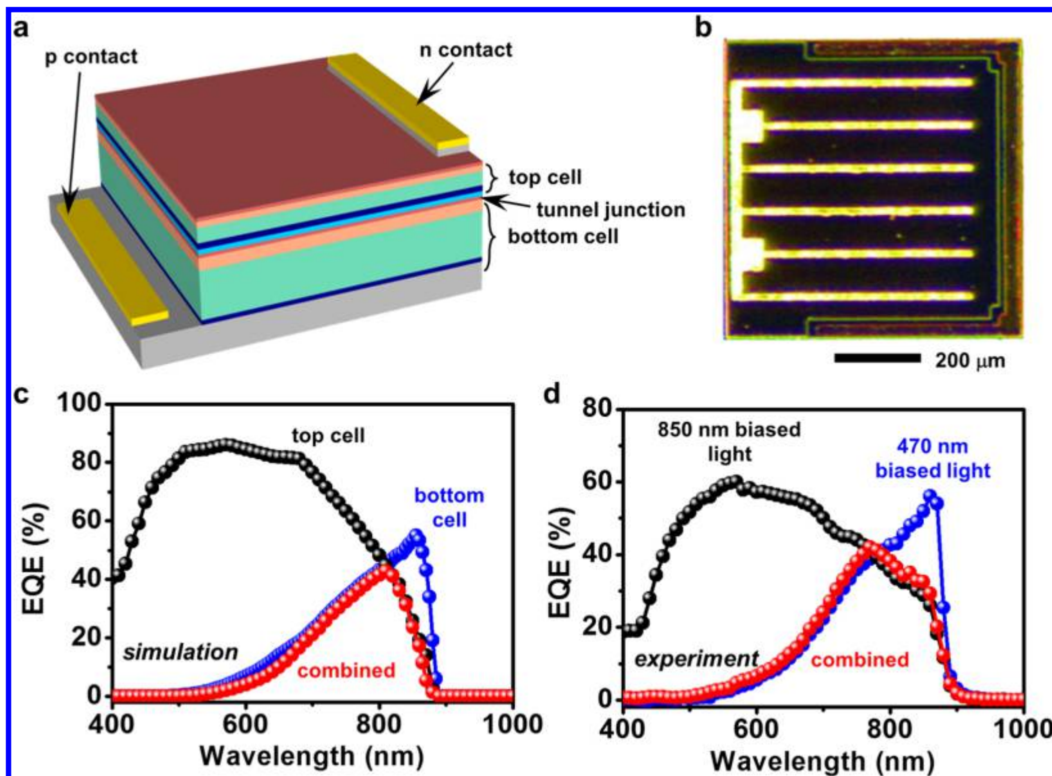

Figure 1. (a) Schematic illustration of the GaAs double-junction photodiode. Different colors represent different materials and structures, including p and n contact layers, a top cell, a tunnel junction, and a bottom cell. (b) Bright-field microscopic image of a fabricated GaAs double-junction photodiode (top view). (c) Simulated and (d) measured external quantum efficiency (EQE) spectra of a GaAs double-junction photodiode and its subcells.

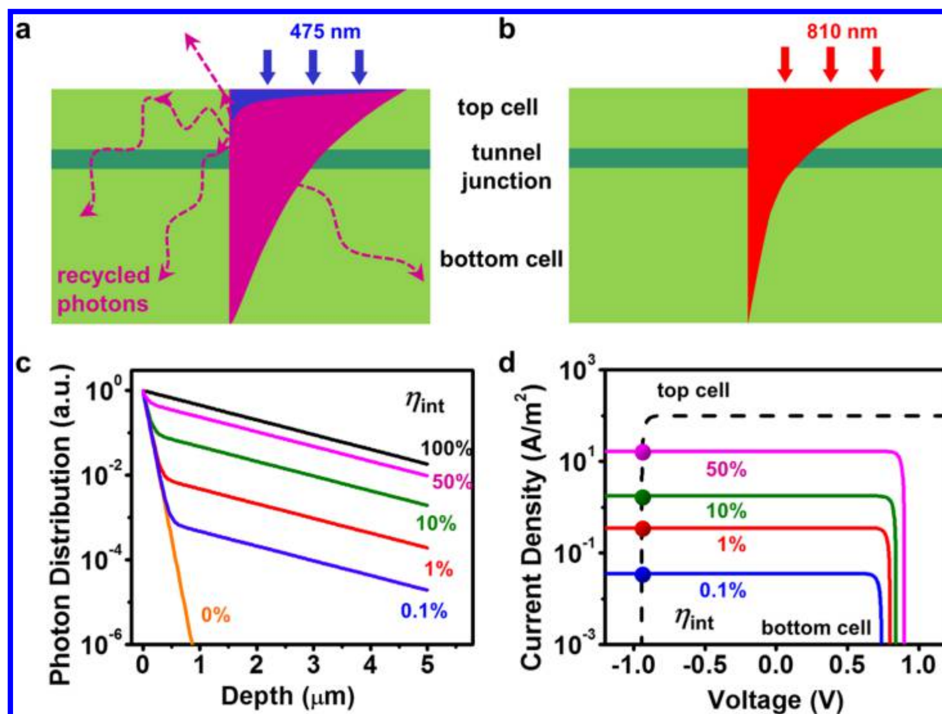

Figure 2. (a,b) Cartoon illustrations of optical processes (absorption and photon-recycling) inside the GaAs double-junction photodiode under (a) 475 and (b) 810 nm light illumination, respectively. (c) Calculated photon distribution inside the device under 475 nm illumination as a function of depth, considering photon-recycling effects with different internal quantum efficiencies (η_{int} = 0, 0.1, 1, 10, 50, and 100%). (d) Calculated current density−voltage characteristics for the top cell (black dashed line) and the bottom cell (colored lines) with corresponding η_{int} (0.1, 1, 10, and 50%). The intersection points represent the working conditions of subcells in the GaAs double-junction photodiode under the short-circuit condition at 475 nm.

DOI: 10.1021/acsphotonics.8b01404
ACS Photonics 2019, 6, 59−65

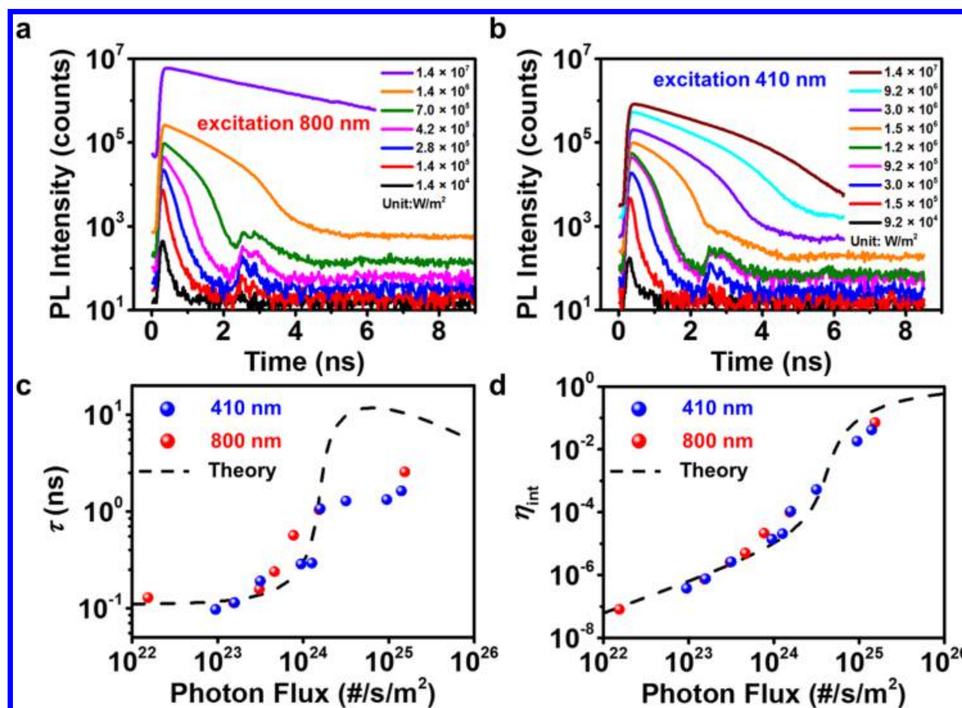

Figure 3. (a,b) Time-resolved photoluminescence (TRPL) decay measured for a GaAs double-junction photodiode under femtosecond laser illumination with different power densities at (a) 800 nm (from top to bottom: 1.4×10^7, 1.4×10^6, 7.0×10^5, 4.2×10^5, 2.8×10^5, 1.4×10^5, and 1.4×10^4 W/m^2) and (b) 410 nm (from top to bottom: 1.4×10^7, 9.2×10^6, 3.0×10^6, 1.5×10^6, 1.2×10^6, 9.2×10^5, 3.0×10^5, 1.5×10^5, and 9.2×10^4 W/m^2), respectively. (c) Measured (scattered dots) carrier lifetime (τ) as a function of absorbed photon flux at 800 (red) and 410 nm (blue) and the theoretical fitting curve (black dashed line). (d) Calculated η_{int} as a function of absorbed photon flux at 800 (red) and 410 nm (blue) based on measured τ in panel c and the theoretical fitting curve (black dashed line).

based tunnel junction. The thicknesses of the top and the bottom GaAs cells are, respectively, designed to be 680 and 1730 nm to realize the current-matching condition and the optimal responsivity at the wavelength of ∼800 nm.[18] Instead of using an indium gallium phosphide (InGaP)/GaAs-based double-junction cell conventionally applied for PV research, here we employ a GaAs/GaAs double-junction photodiode structure because: (1) We optimize the device layers to achieve optimal responses around 800 nm as an efficient near-IR photodetector.[18] (2) GaAs is better for studying photon-recycling processes than InGaP because it has higher internal quantum efficiencies.[19] (3) Serially connected ultrathin GaAs junctions demonstrate high output voltages associated with their more efficient carrier collection compared with the thicker counterpart.[7] (4) Such highly current mismatched dual-junction devices show strong power-dependent photon-recycling processes.[17] The microscale device is lithographically defined, metalized, and chemically released from the original growth substrate, forming a thin-film freestanding GaAs double-junction photodiode that can be integrated onto any foreign substrates. Figure 1b illustrates such a GaAs double-junction photodiode on glass via transfer printing methods,[20−23] with lateral dimensions of 700 × 700 μm^2 and a thickness of 3.8 μm. External quantum efficiency (EQE) spectra of the entire device, the top and the bottom subcells, are calculated based on the finite-element method (Silvaco) and are plotted in Figure 1c. As we designed, the combined device reaches the maximum EQE at ∼800 nm, where each subcell absorbs an equivalent amount of photons, and currents are matched between the cells. At other wavelengths, the combined EQE decreases because the device operation deviates from the current-matching condition, and the overall current is determined by the subcell with a smaller current output. Figure 1d plots the experimental results, in which the EQE spectra of the top and the bottom cells are measured under 850 and 470 nm saturated bias lights, respectively. In this setup, the irradiation intensity of monochromator light is 1−3 mW/cm^2. The experimental and calculated results are in a good agreement, with some discrepancies ascribed to the thickness variation during epi-layer deposition as well as the unwanted carrier losses at the surfaces.

The EQE results of the double-junction photodiode are schematically explained in Figure 2a,b. Here we analyze the device response under monochromatic illuminations with 475 nm blue light (Figure 2a) and 810 nm IR light (Figure 2b) and assume that GaAs is nonluminescent under weak irradiation. On the basis of the Beer−Lambert law,[24] we can calculate the absorbed photon distribution across the device thickness. For GaAs, optical absorption lengths at 475 and 810 nm are about 68 and 769 nm, respectively.[25] At 475 nm, most (>99%) photons are captured and absorbed by the top GaAs cell, generating many more free carriers than the bottom cell does (Figure 2a). When the two subcells are connected in series and measured under the short-circuit condition (V = 0), the negligible overall photocurrent is produced, resulting in an EQE close to zero. By contrast, the IR light at 810 nm can penetrate more deeply into the GaAs layers, leading to a more uniform photon distribution (Figure 2b). Therefore, current matching can be realized, and the maximum EQE is achieved.

However, in highly luminescent materials like GaAs, photons and carriers can be "recycled" via re-emission and reabsorption if they cannot be collected by the external circuit due to current mismatch. Such photon-recycling effects could, in turn, alter the photon distribution inside the device.[17,26−28] As

DOI: 10.1021/acsphotonics.8b01404
ACS Photonics 2019, 6, 59−65

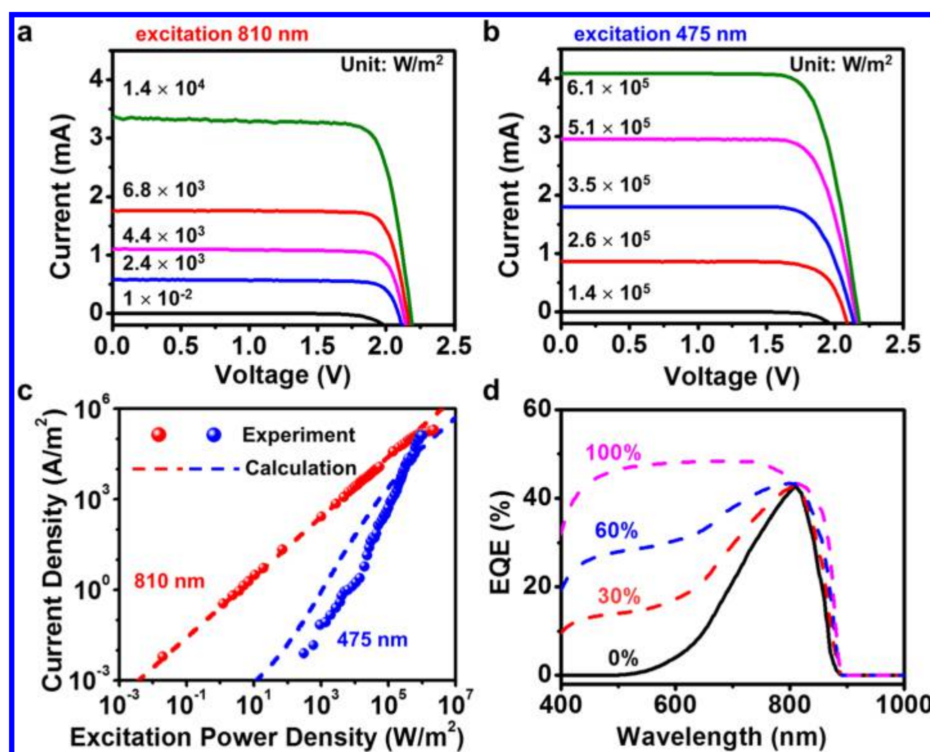

Figure 4. (a,b) Current−voltage curves of a GaAs double-junction photodiode measured under varied illumination power densities at (a) 810 (from top to bottom: 1.4×10^4, 6.8×10^3, 4.4×10^3, 2.4×10^3, and 1×10^{-2} W/m^2) and (b) 475 nm (from top to bottom: 6.1×10^5, 5.1×10^5, 3.5×10^5, 2.6×10^5, and 1.5×10^5 W/m^2), respectively. (c) Measured (scattered dots) and calculated (dashed line) current densities of the GaAs double-junction photodiode as a function of excitation power density at 810 (red) and 475 nm (blue). (d) Conceptual illustrations of the photon-recycling effects on EQE spectra of the double-junction photodiode with different radiative efficiencies (0, 30, 60, and 100%).

illustrated in Figure 2a, photogenerated electrons and holes in the top cell are trapped and undergo recombination via radiative and nonradiative processes. Radiative recombinations create re-emitted photons at the semiconductor band edge (for GaAs, wavelength ~870 nm at room temperature), which redistribute in the entire device, generate photocarriers in both top and bottom cells, and lead to nonzero photocurrent. The varied photon distributions are determined by the radiative efficiencies of GaAs (i.e., internal quantum efficiencies, η_{int}). Figure 2c plots the calculated photon distribution (including both incident photons at 475 nm and re-emitted photons at 870 nm) as a function of depth in GaAs with different η_{int} based on the Beer−Lambert law (details in the Supporting Information S1).[24] When $\eta_{int} = 0$, the illumination is dominated by the 475 nm blue light, with the distribution strictly obeying the Beer−Lambert law. As η_{int} increases, re-emitted photons at 870 nm need to be taken into account, which penetrate into the deeper region due to the reduced absorption coefficient in GaAs. Consequently, the bottom cell operation could be significantly influenced by such photon-recycling processes, as shown in Figure 2d. Here we assume that the 475 nm blue illumination has an incident power of 400 W/m^2 and calculate current−voltage characteristics for each cell in the GaAs double-junction photodiode with different η_{int}. When the combined device (overall current, I, and overall voltage, V) is operated under the short-circuit condition (V = 0), currents and voltages for the two subcells (top cell: I_1, V_1; bottom cell: I_2, V_2) should satisfy

$$I = I_1 = I_2$$
$$V_1 + V_2 = 0 \tag{1}$$

The intersection points in Figure 2d represent the working conditions of the subcells for the GaAs double-junction photodiode at 475 nm. Under these scenarios, the top cell is forward-biased and emits IR photons, whereas the bottom cell receives the recycled IR photons and works at the reverse bias. By contrast, such photon-recycling effects are negligible at the incidence of 810 nm (Figure 2b) because the photogenerated carriers are immediately collected by the external circuit under the current-matching condition.

To reveal the photocarrier dynamics of the device, time-resolved photoluminescence (TRPL) measurements are performed under different excitation wavelengths with a femtosecond laser. Figure 3a,b shows the PL decays of a GaAs double-junction photodiode measured at 800 (power density from 1.4×10^4 to 1.4×10^7 W/m^2) and 410 nm (power density from 9.2×10^4 to 1.4×10^7 W/m^2), respectively. In Figure 3c, the derived PL decay lifetime τ is plotted as a function of photon flux at both wavelengths, in comparison with the fitting curve based on the standard ABC model[29]

$$\tau = \frac{1}{A + B(n_0 + \Delta n) + C\Delta n(n_0 + \Delta n)} \tag{2}$$

where A represents nonradiative recombination and is a function of excess carrier density, B denotes radiative recombination and is assumed to be a constant (1.5×10^{-10} s^{-1} cm^3),[15,30] and C is associated with the Auger recombination and can be neglected at relatively low carrier densities.[31] Detailed analyses are presented in the Supporting Information S2. The differences between the analytical fitting curve and measured data in Figure 3c stem from complicated non-

DOI: 10.1021/acsphotonics.8b01404
ACS Photonics 2019, 6, 59−65

radiative recombination mechanisms (surface defects, deep level traps, etc.), which are difficult to model in eq 2. The internal quantum efficiency (η_{int}) can be expressed as the ratio between the radiative recombination rate (U_{rad}) and the nonradiative recombination rate (U_{nonrad})

$$\eta_{int} = \frac{U_{rad}}{U_{rad} + U_{nonrad}} = \frac{B[(p_0 + \Delta p)(n_0 + \Delta n) - n_i^2]}{A\Delta n + B[(p_0 + \Delta p)(n_0 + \Delta n) - n_i^2]} \quad (3)$$

On the basis of the experimental results of τ, we can calculate η_{int} as a function of photon flux. As shown in Figure 3d, η_{int} monotonically increases with the absorbed photon flux, which is attributed to the gradual saturation of nonradiative recombination centers.

We further measure the current−voltage characteristics of the GaAs double-junction photodiode under varied illumination power densities at 810 (from 0.02 to 2.2×10^6 W/m^2) and 475 nm (from 300 to 10^6 W/m^2), with results, respectively, illustrated in Figure 4a,b. The device exhibits open-circuit voltages of ∼2.0 V, and its photocurrent increases in accordance with the illumination power. The measured current density is plotted in Figure 4c as a function of the excitation power for both 810 (red dots) and 475 nm (blue dots) illuminations. At 810 nm, absorbed photons are nearly equally distributed in each subcell of the GaAs double-junction photodiode. As shown in Figure 1c, calculated photon absorption in both the top cell and the bottom cell is ∼40%. Therefore, the device reaches the current-matching condition, and the output current is linearly proportional to the excitation power (red dashed line)

$$I = I_{ph} \times \mathrm{EQE}\ (\lambda = 810\ \mathrm{nm}) \quad (4)$$

where I_{ph} is the incident photon flux and EQE is ∼40%, as calculated and measured in Figure 1.

By contrast, most of the photons at 475 nm are absorbed by the top cell, and only part of photogenerated carriers produce re-emitted photons that can be recycled by the bottom cell, as explained in Figure 2a. Consequently, the overall current is determined by the cell with a smaller current output, which is the bottom cell in this case (details in the Supporting Information S3). Therefore, the output current is dependent on the photon-recycling efficiency

$$I = \frac{I_{ph}}{1 + \frac{1}{\eta_{LC}}} \quad (5)$$

where η_{LC} is defined as the luminescence coupling efficiency and mainly related to η_{int} as well as the device geometry[11]

$$\eta_{LC} = \frac{\eta_{int}\overline{P_{LC}}}{1 - \eta_{int}\overline{P_{abs}}} \quad (6)$$

where $\overline{P_{abs}}$ and $\overline{P_{LC}}$ are the probabilities of internal photons to be reabsorbed inside the top cell itself and to be coupled to the bottom cell in the GaAs double-junction photodiode, both of which are determined by the cell structures (details in the Supporting Information S4). We can get

$$I = \frac{I_{ph}}{1 + \frac{1 - 0.573\eta_{int}}{0.356\eta_{int}}} \quad (7)$$

By applying the experimentally obtained η_{int} values (Figure 3d) to the above equations, the output current (I) of the GaAs double-junction photodiode can be calculated and plotted in Figure 4c (blue dashed line). The calculation results are consistent with the experiments and exhibit a superlinear relationship with the excitation power density. The remaining discrepancy between experiment and calculated results indicates the existence of additional nonradiative recombination mechanisms in the actual device. Under weak illumination, the photoresponse at 475 nm is orders of magnitude lower than that at 810 nm, in agreement with the measured EQE results in Figure 1d. When the illumination power increases, the photocurrent at 475 nm grows faster than that at 810 nm due to the enhanced photon-recycling effect. Although two monochromatic light sources are used to study the device operation, photon and carrier processes at other wavelengths can be analyzed based on similar principles, depending on the current-match/mismatch states. For such a double-junction device, these results imply that the EQE spectra vary with the illumination intensity at different wavelengths. Figure 4d conceptually predicts such effects based on our observations. Ideally, the EQE spectrum could present a plateau in a wide range when η_{int} approaches 100%, behaving similarly to a single-junction GaAs photodiode but with a doubled output voltage. In this scenario, most free carriers can radiatively recombine and form IR photons that can be recycled by the bottom cell. Therefore, current can be matched between the subcells at most wavelengths. It should be noted that the photon-recycling effect can be diminished at ultrahigh illumination power densities (e.g., for GaAs, >1000 suns) because Auger processes start to dominate the nonradiative recombination.[32]

■ CONCLUSIONS

To summarize, we investigate the optoelectronic performance of a thin-film GaAs-based double-junction photodiode structure and discover that its photoresponse reveals strong illumination and wavelength dependences associated with the photon-recycling effect. It is well known that the photon-recycling effect plays important roles in the V_{oc} and efficiency of single-junction devices. Here we demonstrate that the photon-recycling effect also significantly influences the photocurrent in multijunction devices by altering the photon coupling between the subcells. For PV cells and detectors made of highly luminescent materials like GaAs, these results imply that the measured EQE spectra are influenced by the illumination intensity, and broadband photoresponses (EQE close to 50% from 400 to 800 nm) can be realized under high-power irradiation, even by using highly current mismatched multijunction devices. Considering the photon coupling, optimal device structures are power-dependent (for example, for devices under one-sun illumination vs concentrated sunlight). Besides the material quality, other factors such as electrical fields and optical interfaces are also critical and impact the photon recycling. Similar effects can be explored in devices based on other light emitters including III-Vs, halide perovskites, quantum dots, and so on. We anticipate that the results presented here could provide constructive insights into the design of high-performance photodetectors, PV cells, and optical sensors in general.

DOI: 10.1021/acsphotonics.8b01404
ACS Photonics 2019, 6, 59−65

METHODS AND MATERIALS

Device Fabrication. The GaAs double-junction photodiode structure is grown on a GaAs substrate by using the metal−organic chemical vapor deposition (MOCVD) method. The detailed structure (from top to bottom) consist of an n-type (Si doping, 6×10^{18} cm^{-3}) GaAs contact layer (200 nm), a top cell (30/100/450/100 nm, n-type InGaP window (Si doping, 2×10^{18} cm^{-3})/n-type GaAs emitter (Si doping, 2×10^{18} cm^{-3})/p-type GaAs base (Zn doping, 10^{17} cm^{-3})/p-type $Al_{0.3}Ga_{0.7}As$ BSF (Mg doping, 5×10^{18} cm^{-3})), a highly doped tunnel junction layer (p-type (C doping, 8×10^{19} cm^{-3})/n-type (Se doping, 9×10^{19} cm^{-3}) GaAs, 11/11 nm), a bottom cell (30/100/1500/100 nm, n-type $Al_{0.3}Ga_{0.7}As$ window (Si doping, 2×10^{18} cm^{-3})/n-type GaAs emitter (Si doping, 2×10^{18} cm^{-3})/p-type GaAs base (Zn doping, 10^{17} cm^{-3})/p-type InGaP BSF (Mg doping, 10^{18} cm^{-3})), a p-type GaAs contact layer (Mg doping, 5×10^{18} cm^{-3}, 1000 nm), a sacrificial layer ($Al_{0.95}Ga_{0.05}As$, 500 nm), and the GaAs substrate. All of the layers are lattice-matched to the GaAs substrate. The device is lithographically patterned, and Ge/Ni/Au and Cr/Au serve as ohmic electrodes for n-type and p-type GaAs contact layers, respectively. Freestanding thin-film devices are formed by removing the $Al_{0.95}Ga_{0.05}As$ sacrificial layer in diluted hydrofluoric-acid (HF)-based solution (HF/water 1:10 by volume, with few drops of ethanol). Using patterned poly(dimethylsiloxane) (PDMS) stamps, released devices are picked up and transferred to various carrier substrates (glass, polyimide film, silicon, etc.) with a spin-coated adhesive layer.[20]

Device Characterization. Current−voltage characteristics are recorded using a Keithley 2400 source meter. Illuminations are provided with various light sources, including a 475 nm diode laser (Changchun New Industries Optoelectronics) and an 810 nm diode laser (Hi-Tech Optoelectronics). EQE spectra are measured using an incident photo-to-charge carrier efficiency (IPCE) measurement system (QEX10, PV Measurement, USA) from 400 to 1000 nm, of which the irradiation intensity of monochromator light is 1−3 mW/cm^2. The EQE spectra of the top and bottom subcells are measured with the 850 and 470 nm saturated bias lights (light sources: M850L3-C1 and M470L3-C1 from Thorlabs), respectively.

TRPL measurements are taken using an ultrafast pulse laser from a Spectra-Physics Mai Tai apparatus (410 or 800 nm, 80 MHz, ∼120 fs). The laser spot sizes are ∼80 μm. The emission light passes through an 830 nm long pass filter (BLP01-830R-25, Semrock) and is collected by a single-photon avalanche photodiode detector (TDA 200) combined with a time-correlated single photon-counting module (TimeHarp 260 PICO Single).

ASSOCIATED CONTENT

Supporting Information

The Supporting Information is available free of charge on the ACS Publications website at DOI: 10.1021/acsphotonics.8b01404.

Detailed analytical calculation for short-circuit current (I_{sc}) of GaAs double-junction photodiode by considering the photon-recycling effects (PDF)

AUTHOR INFORMATION

Corresponding Author

*E-mail: xingsheng@tsinghua.edu.cn.

ORCID

Kaihui Liu: 0000-0002-8781-2495

Xing Sheng: 0000-0002-8744-1700

Notes

The authors declare no competing financial interest.

ACKNOWLEDGMENTS

This work is supported by the National Natural Science Foundation of China (grants 51602172 and 61874064). X.S. also acknowledges support from the Beijing Innovation Center for Future Chips, Tsinghua University.

REFERENCES

(1) Green, M. A.; Keevers, M. J.; Thomas, I.; Lasich, J. B.; Emery, K.; King, R. R. 40% efficient sunlight to electricity conversion. *Prog. Photovoltaics* **2015**, *23* (6), 685−691.

(2) Kim, D. Y.; Park, J. H.; Lee, J. W.; Hwang, S.; Oh, S. J.; Kim, J.; Sone, C.; Schubert, E. F.; Kim, J. K. Overcoming the fundamental light-extraction efficiency limitations of deep ultraviolet light-emitting diodes by utilizing transverse-magnetic-dominant emission. *Light: Sci. Appl.* **2015**, *4*, e263.

(3) Martí, A.; Balenzategui, J. L.; Reyna, R. F. Photon recycling and Shockley's diode equation. *J. Appl. Phys.* **1997**, *82* (8), 4067−4075.

(4) Pazos-Outón, L. M.; Szumilo, M.; Lamboll, R.; Richter, J. M.; Crespo-Quesada, M.; Abdi-Jalebi, M.; Beeson, H. J.; Vrućinić, M.; Alsari, M.; Snaith, H. J.; Ehrler, B.; Friend, R. H.; Deschler, F. Photon recycling in lead iodide perovskite solar cells. *Science* **2016**, *351* (6280), 1430−1433.

(5) Miller, O. D.; Yablonovitch, E.; Kurtz, S. R. Strong Internal and External Luminescence as Solar Cells Approach the Shockley−Queisser Limit. *IEEE J. Photovolt.* **2012**, *2* (3), 303−311.

(6) Su, Z. C.; Xu, S. J.; Wang, X. H.; Ning, J. Q.; Wang, R. X.; Lu, S. L.; Dong, J. R.; Yang, H. Effective Photon Recycling and Super Long Lived Minority Carriers in InGaP/GaAs Heterostructure Solar Cell: A Time-Resolved Optical Study. *IEEE J. Photovolt.* **2018**, *8* (3), 820−824.

(7) Proulx, F.; York, M. C. A.; Provost, P. O.; Ares, R.; Aimez, V.; Masson, D. P.; Fafard, S. Measurement of strong photon recycling in ultra-thin GaAs n/p junctions monolithically integrated in high-photovoltage vertical epitaxial heterostructure architectures with conversion efficiencies exceeding 60%. *Phys. Status Solidi RRL* **2017**, *11* (2), 1600385.

(8) Cariou, R.; Benick, J.; Feldmann, F.; Hohn, O.; Hauser, H.; Beutel, P.; Razek, N.; Wimplinger, M.; Blasi, B.; Lackner, D.; Hermle, M.; Siefer, G.; Glunz, S. W.; Bett, A. W.; Dimroth, F. III-V-on-silicon solar cells reaching 33% photoconversion efficiency in two-terminal configuration. *Nat. Energy* **2018**, *3* (7), 606−606.

(9) Green, M. A.; Ho-Baillie, A.; Snaith, H. J. The emergence of perovskite solar cells. *Nat. Photonics* **2014**, *8* (7), 506−514.

(10) Walker, A. W.; Höhn, O.; Micha, D. N.; Bläsi, B.; Bett, A. W.; Dimroth, F. Impact of Photon Recycling on GaAs Solar Cell Designs. *IEEE J. Photovolt.* **2015**, *5* (6), 1636−1645.

(11) Steiner, M. A.; Geisz, J. F.; García, I.; Friedman, D. J.; Duda, A.; Olavarria, W. J.; Young, M.; Kuciauskas, D.; Kurtz, S. R. Effects of Internal Luminescence and Internal Optics on Voc and Jsc of III−V Solar Cells. *IEEE J. Photovolt.* **2013**, *3* (4), 1437−1442.

(12) Sheng, X.; Yun, M. H.; Zhang, C.; Al-Okaily, A. a. M.; Masouraki, M.; Shen, L.; Wang, S.; Wilson, W. L.; Kim, J. Y.; Ferreira, P.; Li, X.; Yablonovitch, E.; Rogers, J. A. Device Architectures for Enhanced Photon Recycling in Thin-Film Multijunction Solar Cells. *Adv. Energy Mater.* **2015**, *5* (1), 1400919.

(13) Kosten, E. D.; Atwater, J. H.; Parsons, J.; Polman, A.; Atwater, H. A. Highly efficient GaAs solar cells by limiting light emission angle. *Light: Sci. Appl.* **2013**, *2* (1), No. e45.

(14) Eisler, C. N.; Abrams, Z. e. R.; Sheldon, M. T.; Zhang, X.; Atwater, H. A. Multijunction solar cell efficiencies: effect of spectral

window, optical environment and radiative coupling. *Energy Environ. Sci.* **2014**, *7* (11), 3600−3605.

(15) Nelson, R. J.; Sobers, R. G. Minority-Carrier Lifetime and Internal Quantum Efficiency of Surface-Free GaAs. *J. Appl. Phys.* **1978**, *49* (12), 6103−6108.

(16) Wang, C. G.; Li, C. Y.; Hasselbeck, M. P.; Imangholi, B.; Sheik-Bahae, M. Precision, all-optical measurement of external quantum efficiency in semiconductors. *J. Appl. Phys.* **2011**, *109* (9), 093108.

(17) Walker, A. W.; Hohn, O.; Micha, D. N.; Wagner, L.; Helmers, H.; Bett, A. W.; Dimroth, F. Impact of photon recycling and luminescence coupling on III-V single and dual junction photovoltaic devices. *J. Photonics Energy* **2015**, *5*, 053087.

(18) Ding, H.; Lu, L. H.; Shi, Z.; Wang, D.; Li, L. Z.; Li, X. C.; Ren, Y. Q.; Liu, C. B.; Cheng, D. L.; Kim, H.; Giebink, N. C.; Wang, X. H.; Yin, L.; Zhao, L. Y.; Luo, M. M.; Sheng, X. Microscale optoelectronic infrared-to-visible upconversion devices and their use as injectable light sources. *Proc. Natl. Acad. Sci. U. S. A.* **2018**, *115* (26), 6632−6637.

(19) Tex, D. M.; Imaizumi, M.; Akiyama, H.; Kanemitsu, Y. Internal luminescence efficiencies in InGaP/GaAs/Ge triple-junction solar cells evaluated from photoluminescence through optical coupling between subcells. *Sci. Rep.* **2016**, *6*, 38297.

(20) Kim, T. I.; Kim, M. J.; Jung, Y. H.; Jang, H.; Dagdeviren, C.; Pao, H. A.; Cho, S. J.; Carlson, A.; Yu, K. J.; Ameen, A.; Chung, H. J.; Jin, S. H.; Ma, Z. Q.; Rogers, J. A. Thin Film Receiver Materials for Deterministic Assembly by Transfer Printing. *Chem. Mater.* **2014**, *26* (11), 3502−3507.

(21) Yoon, J.; Jo, S.; Chun, I. S.; Jung, I.; Kim, H. S.; Meitl, M.; Menard, E.; Li, X. L.; Coleman, J. J.; Paik, U.; Rogers, J. A. GaAs photovoltaics and optoelectronics using releasable multilayer epitaxial assemblies. *Nature* **2010**, *465* (7296), 329−U80.

(22) Sheng, X.; Shen, L.; Kim, T.; Li, L. F.; Wang, X. R.; Dowdy, R.; Froeter, P.; Shigeta, K.; Li, X. L.; Nuzzo, R. G.; Giebink, N. C.; Rogers, J. A. Doubling the Power Output of Bifacial Thin-Film GaAs Solar Cells by Embedding Them in Luminescent Waveguides. *Adv. Energy Mater.* **2013**, *3* (8), 991−996.

(23) Sheng, X.; Bower, C. A.; Bonafede, S.; Wilson, J. W.; Fisher, B.; Meitl, M.; Yuen, H.; Wang, S. D.; Shen, L.; Banks, A. R.; Corcoran, C. J.; Nuzzo, R. G.; Burroughs, S.; Rogers, J. A. Printing-based assembly of quadruple-junction four-terminal microscale solar cells and their use in high-efficiency modules. *Nat. Mater.* **2014**, *13* (6), 593−598.

(24) Swinehart, D. F. The Beer-Lambert Law. *J. Chem. Educ.* **1962**, *39* (7), 333.

(25) Palik, E. D. *Handbook of Optical Constants of Solids*; Academic Press: San Diego, 1998.

(26) Kuriyama, T.; Kamiya, T.; Yanai, H. Effect of Photon Recycling on Diffusion Length and Internal Quantum Efficiency in $Al_xGa_{1-x}As$-GaAs Heterostructures. *Jpn. J. Appl. Phys.* **1977**, *16* (3), 465−477.

(27) Essig, S.; Steiner, M. A.; Allebé, C.; Geisz, J. F.; Paviet-Salomon, B.; Ward, S.; Descoeudres, A.; LaSalvia, V.; Barraud, L.; Badel, N.; Faes, A.; Levrat, J.; Despeisse, M.; Ballif, C.; Stradins, P.; Young, D. L. Realization of GaInP/Si Dual-Junction Solar Cells With 29.8% 1-Sun Efficiency. *IEEE J. Photovolt.* **2016**, *6* (4), 1012−1019.

(28) Ren, Z. K.; Mailoa, J. P.; Liu, Z.; Liu, H. H.; Siah, S. C.; Buonassisi, T.; Peters, I. M. Numerical Analysis of Radiative Recombination and Reabsorption in GaAs/Si Tandem. *IEEE J. Photovolt.* **2015**, *5* (4), 1079−1086.

(29) Schubert, E. F. *Light-Emitting Diodes*; Cambridge University Press: New York, 2006.

(30) Lush, G. B. B-coefficient in n-type GaAs. *Sol. Energy Mater. Sol. Cells* **2009**, *93* (8), 1225−1229.

(31) Steiauf, D.; Kioupakis, E.; Van de Walle, C. G. Auger Recombination in GaAs from First Principles. *ACS Photonics* **2014**, *1* (8), 643−646.

(32) Araujo, G. L.; Marti, A. Limiting Efficiencies of GaAs Solar-Cells. *IEEE Trans. Electron Devices* **1990**, *37* (5), 1402−1405.

DOI: 10.1021/acsphotonics.8b01404
ACS Photonics 2019, 6, 59−65

Supporting Information for

Power- and Spectral-Dependent Photon-Recycling Effects in a Double-Junction Gallium Arsenide Photodiode

He Ding[1], Hao Hong[2], Dali Cheng[3], Zhao Shi[3], Kaihui Liu[2], Xing Sheng[3,*]

[1]School of Optics and Photonics, Beijing Institute of Technology, Beijing 100081, China

[2]State Key Laboratory for Mesoscopic Physics, Collaborative Innovation Center of Quantum Matter, and School of Physics, Peking University, Beijing 100871, China

[3]Department of Electronic Engineering, Tsinghua University, Beijing 100084, China

* Correspondence to: xingsheng@tsinghua.edu.cn

Contents:

S1. Photon distribution

S2. Carrier Recombination

S3. Luminescence coupling efficiency of the GaAs double junction photodiode

S4. Short-circuit current of the GaAs double junction photodiode

We analytically calculate the relationship between short-circuit current (I_{sc}) of GaAs double junction photodiode and excitation power density (P), considering the photon-recycling effects.

S1. Photon Distribution

The photon distribution is calculated based on a phenomenological approach using the absorption coefficient (α) of GaAs at 475 nm (excitation wavelength, $\alpha = 1.511\times10^7$ m^{-1}) and 870 nm (band edge of GaAs, $\alpha = 8\times10^5$ m^{-1}).[1] A semi-infinitely large semiconductor bulk (thickness: z from 0 to ∞) is assumed, and we calculate the number of photons both at wavelength of 475 nm (N_{475}) and 870 nm (N_{870}) as a function of the thickness.

The photons at a wavelength of 475 nm derive from the external irradiation light, which is conformed to the Beer–Lambert Law[2]:

$$N_{475}(z) = N_{475}^{0} \exp(-\alpha_{475} z) \qquad (1)$$

The photons at a wavelength of 475 nm derive from the photon-recycling effect, which is initially generated by the photons at a wavelength of 475 nm and related to the internal quantum efficiency (η_{int}) of the material.

$$\begin{aligned} \mathrm{d}N_{870}(z) &= -\eta_{\text{int}} \mathrm{d}N_{475}(z) - \alpha_{870} N_{870}(z)\mathrm{d}z \\ N_{870}(z) &= N_{475}^{0} \frac{\alpha_{475}}{\alpha_{475} - \alpha_{870}} \eta_{\text{int}} \left(\exp(-\alpha_{870} z) - \exp(-\alpha_{475} z) \right) \end{aligned} \qquad (2)$$

And the total photon distribution is sum of the N_{475} and N_{870}:

$$N(z) = N_{475}(z) + N_{870}(z)$$
$$= \frac{\alpha_{475}}{\alpha_{475} - \alpha_{870}} N_{475}^{0} \left(\eta_{\text{int}} \exp(-\alpha_{870} z) + \left(1 - \eta_{\text{int}} - \frac{\alpha_{870}}{\alpha_{475}} \right) \exp(-\alpha_{475} z) \right) \tag{3}$$

Furthermore, as the tremendous differences of α between the wavelength of 870 nm and 475 nm ($\alpha_{870} / \alpha_{475} \approx 0$), the photon distribution can be further simplified as:

$$N(z) = N_{475}^{0} \left(\eta_{\text{int}} \exp(-\alpha_{870} z) + \left(1 - \eta_{\text{int}} \right) \exp(-\alpha_{475} z) \right) \tag{4}$$

which is a linear combination of the Beer−Lambert law for the wavelength of 870 nm and 475 nm.

S2. Carrier Recombination

In the ABC model, the carrier recombination rate (R) in a bulk semiconductor material is expressed with the carrier density (n):

$$R = An + Bn^2 + Cn^3 \tag{5}$$

In this model, the SRH recombination is represented by coefficient A (or its reciprocal, nonradiative carrier lifetime, τ_{nr}).[3–5] Thus, τ_{nr} can be expressed as:

$$\tau_{\text{nr}} = \frac{1}{A} = \left(\tau_{\text{p0}} \frac{n_0 + n_1}{n_0 + p_0} + \tau_{\text{n0}} \frac{p_0 + p_1}{n_0 + p_0} \right) \frac{1 + \frac{\Delta n \left(\tau_{\text{p0}} + \tau_{n0} \right)}{\tau_{\mathbf{p}0} \left(n_0 + n_1 \right) + \tau_{n0} \left(p_0 + p_1 \right)}}{1 + \frac{\Delta n}{n_0 + p_0}} \tag{6}$$

where n_0 and p_0 are electron and hole equilibrium density, Δn is excess carrier density, τ_{p0} and τ_{n0} are two lifetime constants (unrelated to carrier density), n_1 and p_1 are defined as following if E_t is the trap energy level:

$$n_1 = N_C \exp\left(-\frac{E_C - E_t}{kT}\right)$$
$$p_1 = N_V \exp\left(-\frac{E_t - E_V}{kT}\right) \quad (7)$$

In general, n_0 is relatively large and p_0 is very small in an n-type semiconductor.[3] If the trap energy level E_t is in the middle of the bandgap, n_1 and p_1 can also be negligible. Therefore, the formula above can be simplified to

$$\tau_{nr} = \frac{1}{A} = \frac{\tau_{p0} + \frac{\Delta n}{n_0}\left(\tau_{p0} + \tau_{n0}\right)}{1 + \frac{\Delta n}{n_0}} \quad (8)$$

When Δn is zero, $\tau_{nr} = \tau_{p0}$, which equals to the minority carrier nonradiative lifetime. When Δn approaches infinity, $\tau_{nr} = \tau_{p0} + \tau_{n0}$, which is the sum of the majority and the minority carrier nonradiative lifetime. In general, as Δn is monotonously dependent on τ_{nr}, the coefficient A gets smaller at higher excitation levels.

And the radiative recombination process is represented by coefficient B in this model, which is mainly determined by temperature (T) and the absorption coefficient (α):

$$B = \frac{8\pi}{h^3 c_0^2 n_i^2} \int_0^\infty n^2 \left(h\nu\right)^2 \alpha\left(h\nu, T\right) \exp\left(-\frac{h\nu}{kT}\right) \mathrm{d}\left(h\nu\right) \quad (9)$$

For GaAs at the temperature of 300 K, the coefficient B is assumed to be independent of carrier density n, and is set to be a constant 1.5×10^{-10} cm^3 s^{-1}.[5, 6]

The Auger recombination process, which is represented by coefficient C, consists of the conduction-band Auger process (CHCC) and the valence-band Auger process (CHSH). For CHCC, the Auger coefficient is determined by the related band structure (and vice versa for CHSH), and can be expressed as:

$$C = \frac{4\pi^{1/2}h^2 g(E) e^4 F}{(2m_v kT)^{3/2}} \frac{k_0^2}{E_c(k_0) - E_v(k_0)} \exp\left(-\frac{E_v(k_0)}{kT}\right) \tag{10}$$

where $g(E)$ is the state density function, and k_0 is the wave vector in the conduction band.[7] In most scenarios, the Auger recombination coefficient (C) of GaAs is normally smaller than 10^{-30} cm^6 s^{-1}, so the influence of Auger recombination can be neglected if the carrier density is lower than 10^{20} cm^{-3}.[8–11] Thus, the coefficient C is negligible in this analysis due to the low excitation power density ($P < 1.4\times10^7$ W/m^2) and the corresponding low carrier density ($n < 10^{18}$ cm^{-3}).

S3. Luminescence coupling efficiency of the GaAs double junction photodiode

Under steady state condition, the carrier generation rate and the total recombination rate should be equal. Assuming a uniform distribution of carriers in the top cell, the excess carrier density is determined by the excitation power density:

$$A\Delta n + B\left[\left(p_0 + \Delta p\right)\left(n_0 + \Delta n\right) - n_{\mathrm{i}}^2\right] = \frac{P}{h\nu L_1} \qquad (11)$$

where $\Delta n=\Delta p$ is the excess carrier density, p_0 and n_0 are equilibrium carrier densities, n_{i} is the intrinsic carrier density, P is the incident power density, v is the frequency of incident light, and L_1 is the thickness of the top cell (cell 1). As IQE (η_{int}) is the ratio of the radiative recombination rate and the total recombination rate, η_{int} can be expressed as a function of excitation power density:

$$\eta_{\mathrm{int}}\left(P\right) = \frac{U_{\mathrm{rad}}}{U_{\mathrm{rad}} + U_{\mathrm{nonrad}}} = \frac{B\left[\left(p_0 + \Delta p\left(P\right)\right)\left(n_0 + \Delta n\left(P\right)\right) - n_{\mathrm{i}}^2\right]}{A\Delta n\left(P\right) + B\left[\left(p_0 + \Delta p\left(P\right)\right)\left(n_0 + \Delta n\left(P\right)\right) - n_{\mathrm{i}}^2\right]} \qquad (12)$$

Furthermore, by taking reference of the model in Ref.[12], the luminescence coupling efficiency (η_{LC}) in the GaAs double junction photodiode can be written as:

$$\eta_{\mathrm{LC}}\left(P\right) = \frac{\eta_{\mathrm{int}}\left(P\right)\overline{P_{\mathrm{LC}}}}{1-\eta_{\mathrm{int}}\left(P\right)\overline{P_{\mathrm{abs}}}} \qquad (13)$$

where $\overline{P_{\mathrm{abs}}}$ and $\overline{P_{\mathrm{LC}}}$ are the probabilities of internal photons to be reabsorbed inside the top cell itself and to be coupled to the bottom cell in the GaAs double junction photodiode. They are determined by the optical properties of the GaAs double junction photodiode and the substrate index:

$$\begin{aligned}
\overline{P_{\mathrm{abs}}} &= 1 - \int_0^{\frac{\pi}{2}} \frac{1-\exp\left(-\frac{\alpha L_1}{\cos\theta}\right)}{\alpha L_1}\left(1 - \frac{R_{\mathrm{f}}\left(\theta\right)}{2}\left(1-\exp\left(-\frac{\alpha L_1}{\cos\theta}\right)\right)\right)\cos\theta\sin\theta\,\mathrm{d}\theta \\
\overline{P_{\mathrm{LC}}} &= \int_0^{\frac{\pi}{2}} \frac{T_{\mathrm{b}}^{'}\left(\theta\right)\exp\left(-\frac{\alpha L_1}{\cos\theta}\right)}{2\alpha L_1}\left(1 + R_{\mathrm{f}}\left(\theta\right)\exp\left(-\frac{\alpha L_1}{\cos\theta}\right)\right)\sin\theta\cos\theta\,\mathrm{d}\theta
\end{aligned} \qquad (14)$$

where α is the absorption coefficient of GaAs at its bandgap (870 nm, 8×10^{5} m^{-1}), $R_{\mathrm{f}}(\theta)$ is the coefficient of reflection that occurs at the top cell-air interface (equals 1 when $\theta < \sin^{-1}(1/n_{\mathrm{GaAs}})$ and otherwise 0) and $T_{\mathrm{b}}^{'}(\theta)$ is the coefficient of transmission that occurs at the interface between two subcells, without counting the absorption in the substrate.[12] So, it can be numerically calculated that $\overline{P_{\mathrm{abs}}}$ and $\overline{P_{\mathrm{LC}}}$ of the GaAs double junction photodiode are 57.3% and 35.6%, respectively.

S4. Short-circuit current of the GaAs double junction photodiode

Based on the detailed balance (DB) theory,[13, 14] the current of the diode is equal to the difference between generated carriers and recombined carriers:

$$I = I_{\mathrm{generation}} - I_{\mathrm{recombination}} = I_{\mathrm{ph}} + I_{\mathrm{th}} - I_{\mathrm{rad}} - I_{\mathrm{nrad}} \qquad (15)$$

where the J_{ph} is the photogenerated current and derived from the incident photons (I_{inc}), I_{th} is the absorbed thermal radiation from the environment, and the I_{rad} is the radiative current, and I_{nrad} is the nonradiative current, and these currents in the device (surface area: S) can be expressed in the following equations:

$$I_{\mathrm{ph}} = \eta_{\mathrm{abs}} I_{\mathrm{inc}} \qquad (16)$$

$$I_{\mathrm{th}} = \frac{2\pi\left(n^{2}+1\right)qkTS}{h^{3}c^{2}} E_{\mathrm{g}}^{2} \exp\left(-\frac{E_{\mathrm{g}}}{kT}\right) \qquad (17)$$

$$I_{\text{rad}} = \frac{2\pi\left(n^2+1\right)qkTS}{h^3c^2}E_{\text{g}}^2\exp\left(\frac{qV-E_{\text{g}}}{kT}\right) \tag{18}$$

$$I_{\text{rad}} = I_{\text{th}}\exp\left(\frac{qV}{kT}\right) \tag{19}$$

As the external radiative efficiency (η_{ext}) is defined as:

$$\eta_{\text{ext}} = \frac{I_{\text{rad}}}{I_{\text{rad}}+I_{\text{nrad}}} \tag{20}$$

The output current can be shorted to:

$$\begin{aligned} I &= I_{\text{ph}} + I_{\text{th}} - I_{\text{rad}} - I_{\text{nrad}} \\ &= I_{\text{ph}} + I_{\text{th}} - I_{\text{rad}}/\eta_{\text{ext}} \\ &= I_{\text{ph}} + I_{\text{th}} - I_{\text{th}}\exp\left(\frac{qV}{kT}\right)/\eta_{\text{ext}} \end{aligned} \tag{21}$$

For the GaAs double junction photodiode irradiated under blue light (475 nm), only the top cell (cell 1, I_1, V_1) is able to receive the incident light and generate the photocarriers, so the

$$I_1 = I_{\text{ph}} + I_{\text{th}} - I_{\text{th}}\exp\left(\frac{qV_1}{kT}\right)/\eta_{\text{ext}} \tag{22}$$

Similarly, considering the bottom cell (cell 2, I_2, V_2) can only receive those photons regenerated by electron-hole radiative recombination in the top cell (photon-recycling effect), the current of the bottom cell can be expressed as:

$$I_2 = I_{\text{ph_1}\rightarrow 2} + I_{\text{th}} - I_{\text{th}}\exp\left(\frac{qV_2}{kT}\right)/\eta_{\text{ext}} \tag{23}$$

Here, the $I_{\text{ph_1}\rightarrow 2}$ is the photocurrent generated by the irradiation based on the photon-recycling effect from the top layer, and is determined by η_{LC}:

$$I_{\mathrm{ph_1\to 2}} = (\eta_{\mathrm{LC}}/\eta_{\mathrm{ext}}) I_{\mathrm{1_rad}} = (\eta_{\mathrm{LC}}/\eta_{\mathrm{ext}}) I_{\mathrm{th}} \exp\left(\frac{qV_1}{kT}\right) \quad (24)$$

By taking into account the series connection restrictions, the current and voltage of the subcells can be expressed as:

$$\begin{aligned} I &= I_1 = I_2 \\ V_1 + V_2 &= 0 \end{aligned} \quad (25)$$

Furthermore, the thermal current I_{th} is negligible compared to J_{ph}. So, the short-circuit current (I_{sc}) of the GaAs double junction photodiode can be simplified as:

$$I_{\mathrm{sc}}(P) = \frac{I_{\mathrm{ph}}(P)}{1 + \frac{1}{\eta_{\mathrm{LC}}(P)}} \quad (26)$$

References

1. Palik, E. D., *Handbook of Optical Constants of Solids*. Academic Press: San Diego, 1998.

2. Swinehart, D. F., The Beer−Lambert Law. *J. Chem. Educ.* **1962,** *39* (7), 333.

3. Neamen, D. A., *Semiconductor physics and devices*. McGraw-Hill: New York, 1997.

4. Schubert, E. F., *Light-emitting diodes*. Cambridge Univ Press: New York, 2006.

5. Lush, G. B., B-coefficient in n-type GaAs. *Sol. Energy Mater. Sol. Cells* **2009,** *93* (8), 1225-1229.

6. Nelson, R. J.; Sobers, R. G., Minority-Carrier Lifetime and Internal Quantum Efficiency of Surface-Free GaAs. *J. Appl. Phys.* **1978,** *49* (12), 6103-6108.

7. Haug, A., Auger recombination in InGaAsP. *Appl. Phys. Lett.* **1983,** *42* (6), 512-514.

8. Strauss, U.; Ruhle, W. W.; Kohler, K., Auger Recombination in Intrinsic Gaas. *Appl. Phys. Lett.* **1993,** *62* (1), 55-57.

9. Mclean, D. G.; Roe, M. G.; Dsouza, A. I.; Wigen, P. E., Picosecond Recombination of Charged Carriers in GaAs. *Appl. Phys. Lett.* **1986,** *48* (15), 992-993.

10. Haug, A., Auger Recombination in Direct-Gap Semiconductors - Band-Structure Effects. *J. Phys. C: Solid State Phys.* **1983,** *16* (21), 4159-4172.

11. Steiauf, D.; Kioupakis, E.; Van de Walle, C. G., Auger Recombination in GaAs from First Principles. *ACS Photonics* **2014,** *1* (8), 643-646.

12. Steiner, M. A.; Geisz, J. F.; García, I.; Friedman, D. J.; Duda, A.; Olavarria, W. J.; Young, M.; Kuciauskas, D.; Kurtz, S. R., Effects of Internal Luminescence and Internal Optics on Voc and Jsc of III–V Solar Cells. *IEEE J. Photovolt.* **2013,** *3* (4), 1437-1442.

13. Shockley, W.; Queisser, H. J., Detailed Balance Limit of Efficiency of P-N Junction Solar Cells. *J. Appl. Phys.* **1961,** *32* (3), 510-519.

14. Martí, A.; Balenzategui, J. L.; Reyna, R. F., Photon recycling and Shockley's diode equation. *J. Appl. Phys.* **1997,** *82* (8), 4067-4075.